Journal of Solid State Chemistry **149,** 252–255 (2000)
doi:10.1006/jssc.1999.8524, available online at http://www.idealibrary.com on IDEAL®

An Mn–K Edge XAS Investigation on the Crystal Chemistry of $Cd_{1-\delta}Mn_2O_y$

P. Ghigna,[1] G. Flor, and G. Spinolo

INSTM, CSTE/CNR, and Dipartimento di Chimica Fisica, Università di Pavia, Viale Taramelli 16, I-27100, Pavia, Italy

Received July 22, 1999; in revised form September 20, 1999; accepted October 11, 1999

XAS spectra recorded at the Mn–K edge show that cadmium manganese spinels, when prepared with a cadmium defect, have Mn(II) substituting Cd in the tetrahedral sites. Thus, the cation distribution can be written as $Cd_{1-x}{}^{t}Mn(II)_x{}^{t}Mn(III)_2{}^{o}O_4$, where t and o refer to the tetrahedral and octahedral sites of the spinel structure, respectively. The lowest and highest cadmium content here investigated correspond to $x = 0.5$ and $x = 0.03$, respectively, but, the solubility range likely extends beyond this range.

1. INTRODUCTION

The $CdMn_2O_4$ spinel is a promising material for mixed potential electrochemical sensors of oxygenic gases such as NO_x (1–3). However, besides the crystal structure, which is a tetragonal distortion (linnaeite-like) of the regular spinel structure (4–6), very limited information can be found in the literature about this compound. As a part of a more complete investigation on materials for gas sensing devices, our group has started research on this compound, aiming at clarifying its electrical properties. A stoichiometric $CdMn_2O_4$ spinel was found hard to obtain, because sol–gel synthesis starting from citrate precursors is ineffective. On the other hand, at the high temperature required by the solid-state synthesis from the parent oxides, CdO has a considerable vapor pressure: the final material was always found to be Cd deficient. An efficient synthetic procedure has been developed by performing the solid-state synthesis starting from CdO and Mn_2O_3 at 800°C in a closed quartz ampoule (7). The procedure gives a monophasic material with known and tunable Cd content, which for the moment will be referred to as $Cd_{1-\delta}Mn_2O_y$. The aim of this work is the elucidation of the cation arrangement of this material, by the application of X-ray absorption spectroscopy (XAS).

[1] To whom correspondence should be addressed at Dipartimento di Chimica Fisica, Università di Pavia, Viale Taramelli 16, I-27100, Pavia, Italy. Fax: + 39 (0) 382 507 575. E-mail: paolo@chifis.unipv.it.

2. EXPERIMENTAL

$Cd_{1-\delta}Mn_2O_y$ materials with $\delta = 0.05$, 0.2, 0.3, 0.6 were synthesized by solid-state reaction starting from stoichiometric amounts of CdO (Aldrich, 99.5%) and Mn_2O_3 (Aldrich, 99%). The powders were suspended in acetone and stirred overnight. After acetone evaporation, the powder mixture was isostatically pressed into pellets and allowed to react at 800°C in a closed quartz ampoule for a total of 90 h with several intermediate grinding and repressing steps.

The XAS Mn–K edge spectra of high-purity MnO, Mn_3O_4, Mn_2O_3, and MnO_2 (Aldrich 99.99%) and of the $Cd_{1-\delta}Mn_2O_y$ sequence were collected at station BM 29 of the ESRF synchrotron radiation laboratory (Grenoble, France). The spectra were collected at room temperature in transmission mode, using ion chambers as detectors and a double-crystal Si(111) monochromator. For the measurement, an amount of sample appropriate to give an edge jump of about 1 in the absorption coefficient was mixed with polyethylene and then pressed into a pellet. For the XANES analysis, the spectra were processed by subtracting the smooth pre-edge background fitted with a straight line and normalized to unit absorption at 7500 eV, where the EXAFS oscillations are not visible anymore. The EXAFS analysis was performed by means of the GNXAS package (8, 9).

X-ray powder diffraction and SEM and EMPA inspections were performed with a Philips 1710 diffractometer equipped with a Cu anticathode and with a JEOL JXA-840A scanning electron microscope, respectively. According to these techniques, the synthetic procedure gave single-phase materials, which were also homogeneous in the chemical composition. As an illustration, the XRPD pattern of the $Cd_{0.80}Mn_2O_y$ material is shown in Fig. 1. The precise determination of the oxygen content and of its variations with temperature and oxygen partial pressure will be the object of a future work. Preliminary estimates have been carried out by thermogravimetric analysis with a 951 Thermogravimetric Analyzer attachment of a TA

0022-4596/00 $35.00

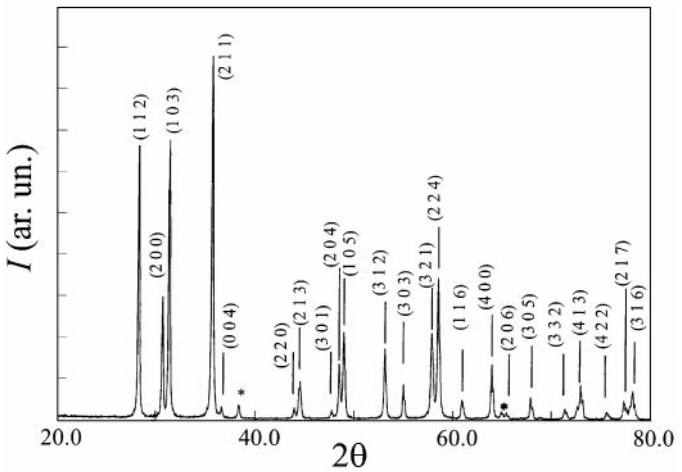

FIG. 1. XRPD pattern of $Cd_{0.80}Mn_2O_y$. The indexing has been made according to JCPDS-ICCD 23-826. The peaks marked with asterisks are due to the aluminum sample holder.

2000 system: y was found to be very close to 4 for all the samples.

3. RESULTS

The XANES spectra at the Mn–K edge of MnO, Mn_3O_4, Mn_2O_3, and MnO_2 and of the $Cd_{1-\delta}Mn_2O_y$ ($\delta = 0.05$ to 0.6) sequence are shown in Fig. 2. The threshold energy E_0, as determined from the first inflection point on the edge, is reported for all the compounds in Table 1 and shows a shift with changes in the Mn oxidation state. This so-called chemical shift is related to the increase in the core-level binding energy with increasing oxidation state, which is in turn caused by the reduced screening of the core level by valence electrons. Thus, the energy position of the edge can be used for evaluating the oxidation state of Mn in the $Cd_{1-\delta}Mn_2O_y$ sequence. From Table 1, it is apparent that, with decreasing Cd content, there is a decrease of the Mn oxidation state from a state close to III to a state intermediate between II and III. It should be remarked that here it is only the relative energy position that is relevant, as the actual exact energy position of an X-ray absorption spectrum can depend also on instrumental factors: as all the spectra were recorded successively on the same beamline and with the same monochromator, which are known to have a very high stability, the reported E_0 sequence can be considered highly reliable.

Figure 3 displays on an enlarged scale the pre-edge parts of the absorption spectra for Mn_3O_4, $Cd_{0.4}Mn_2O_y$, and $Cd_{0.95}Mn_2O_y$. The pre-edge peak originated from the $1s \rightarrow 3d$ transition, which is dipole forbidden but quadrupole allowed. It is therefore more intense for local symmetries lacking an inversion center, where d–p mixing is

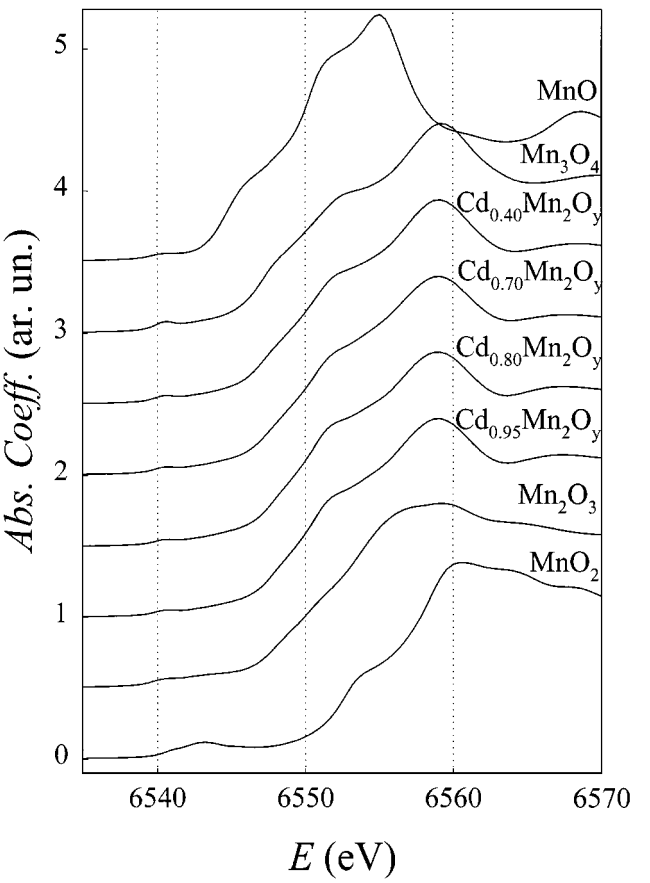

FIG. 2. Mn–K-edge XANES spectra of MnO, Mn_3O_4, Mn_2O_3, MnO_2, $Cd_{0.4}Mn_2O_y$, $Cd_{0.7}Mn_2O_y$, $Cd_{0.8}Mn_2O_y$, and $Cd_{0.95}Mn_2O_y$. For better clarity, the spectra have been arbitrarily shifted along the vertical scale.

permitted. $CdMn_2O_4$ and Mn_3O_4 are known to have the same tetragonally distorted spinel structure (4–6). Although tetragonally elongated, the octahedral sites of both spinels are centrosymmetric. In addition, they are generally

TABLE 1
Threshold Energy E_0, as Determined from the First Inflection Point on the Edge for MnO, Mn_3O_4, MnO_2, $Cd_{0.4}Mn_2O_y$, $Cd_{0.7}Mn_2O_y$, $Cd_{0.8}Mn_2O_y$, and $Cd_{0.95}Mn_2O_y$

Compound	E_0 (eV)
MnO	6544.7
Mn_3O_4	6547.1
$Cd_{0.40}Mn_2O_y$	6547.2
$Cd_{0.70}Mn_2O_y$	6547.8
$Cd_{0.80}Mn_2O_y$	6547.9
$Cd_{0.95}Mn_2O_y$	6547.9
Mn_2O_3	6548.2
MnO_2	6552.6

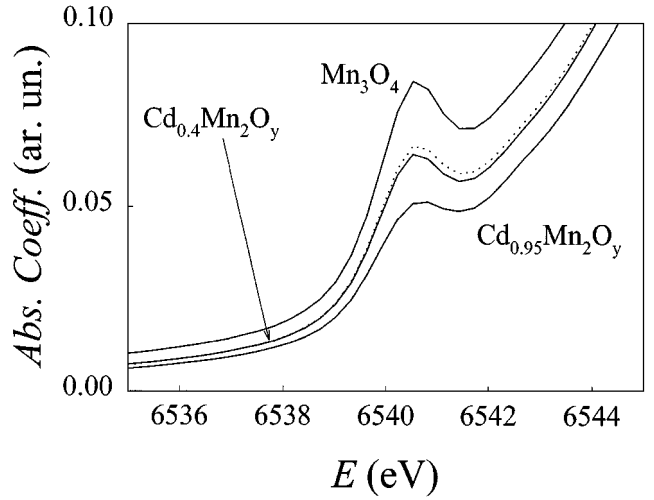

FIG. 3. Pre-edge part of the XANES spectra for Mn_3O_4, $Cd_{0.4}Mn_2O_y$, and $Cd_{0.95}Mn_2O_y$ (full lines). The dotted line is an average of the spectra of Mn_3O_4 and $Cd_{0.95}Mn_2O_y$.

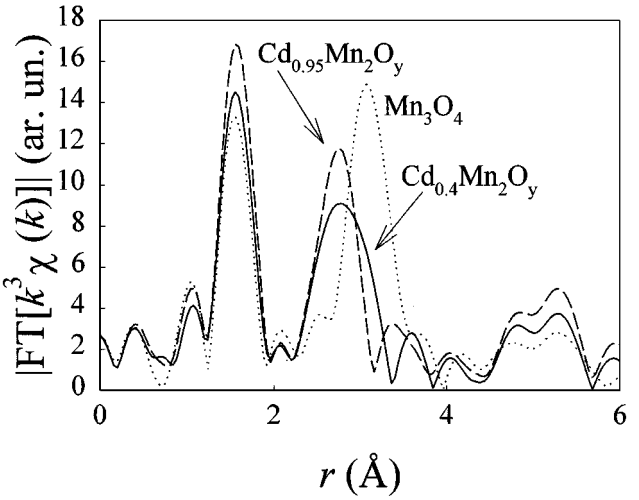

FIG. 5. Fourier transforms (modulus) of the EXAFS spectra of the previous figure.

reported as having no significant inversion disorder (10, 11) and can be written as $Cd^tMn_2{}^oO_4$ and $Mn(II)^tMn(III)_2{}^oO_4$, respectively, where t and o refer to the tetrahedral and octahedral sites of the spinel structure. The marked increase in the prepeak intensity with decreasing Cd content can be therefore nicely accounted for with the presence of Mn in the tetrahedral sites of the reference $CdMn_2O_4$ spinel structure.

The EXAFS spectra for $Cd_{0.4}Mn_2O_y$, $Cd_{0.95}Mn_2O_y$ and for Mn_3O_4 are shown in Fig. 4. Not only are Mn_3O_4 and $CdMn_2O_4$ isostructural but their lattice constants are also very close to each other. It is therefore possible to compare

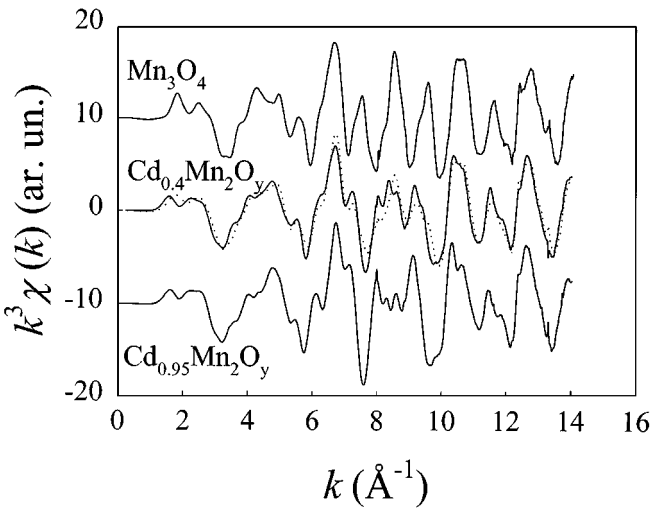

FIG. 4. EXAFS spectra for Mn_3O_4, $Cd_{0.4}Mn_2O_y$, and $Cd_{0.95}Mn_2O_y$ (full lines). The dotted line is an average of the spectra of Mn_3O_4 and $Cd_{0.95}Mn_2O_y$.

directly the EXAFS Fourier transforms (Fig. 5). For both compounds the first shell (i.e., the peaks between 1 and 2 Å in the EXAFS Fourier transforms, the peaks at lower distance being due to some residual post-edge background) is made up of oxygen ions (nearest neighbors of Mn) while the second shell (peaks between 2 and 4 Å) mainly reflects the distance between cations in different (tetrahedral and octahedral) sites. The differences between $Cd_{0.95}Mn_2O_y$ and Mn_3O_4 are due to the fact that the latter material contains only Mn–Mn contributions while the former contains almost only Mn–Cd contributions. The different phase shifts of Cd and Mn cause the apparent displacement toward higher distances of the second coordination shell in Mn_3O_4. As is apparent, the second peak in the EXAFS Fourier transform for $Cd_{0.4}Mn_2O_y$ is somehow intermediate with respect to Mn_3O_4 and $Cd_{0.95}Mn_2O_y$. This experimental finding is further support for the conclusion that there is a partial Mn occupation in the tetrahedral sites of the spinel structure of $CdMn_2O_4$ at low Cd content.

4. DISCUSSION AND CONCLUSIONS

The above-reported experimental results point out the presence of some Mn(II) in the tetrahedral sites of the spinel structure of $CdMn_2O_4$, when the Cd/Mn ratio is below 0.5. Considering that Mn_3O_4 and $CdMn_2O_4$ have the same tetragonally distorted spinel crystal structure, that both compounds are direct spinels, with no significant inversion disorder, and that the lattice constants are quite close to each other ($a = 5.762$, $c = 9.450$ for Mn_3O_4, $a = 5.832$, $c = 9.754$ for $CdMn_2O_4$), one can infer that Mn_3O_4 and $CdMn_2O_4$ are able to originate a range of solid solutions that ideally require no vacancies in the tetrahedral sites. The

common formula of these solutions can be written as $Cd_{1-x}{}^{t}Mn(II)_x{}^{t}Mn(III)_2{}^{o}O_4$: the compounds with minimum and maximum Cd content can then be written as $Cd_{0.5}{}^{t}Mn(II)_{0.5}{}^{t}Mn(III)_2{}^{o}O_4$ and $Cd_{0.97}{}^{t}Mn(II)_{0.03}{}^{t}Mn(III)_2{}^{o}O_4$, respectively. It should be noted that there is no reason to regard these as limiting compositions, and the homogeneity range is probably larger.

The raw XAS data previously reported allow a nice test of these assumptions. In fact, neglecting the small amount of Mn(II) which is contained in $Cd_{0.97}{}^{t}Mn(II)_{0.03}{}^{t}Mn(III)_2{}^{o}O_4$, according to the above assumptions one would obtain the spectrum of $Cd_{0.5}{}^{t}Mn(II)_{0.5}{}^{t}Mn(III)_2{}^{o}O_4$ by averaging those of Mn_3O_4 and $Cd_{0.97}{}^{t}Mn(II)_{0.03}{}^{t}Mn(III)_2{}^{o}O_4$. Such an average is reported as a dotted line both in Fig. 3 for the prepeak and in Fig. 4 for the EXAFS. The prepeak is reproduced in a quite good way by the average, and the agreement between calculated and experimental EXAFS is sensible. It should be noted that also the whole XANES is reproduced very well by the average.

Thus, the assumption of a Cd–Mn mixed occupation of the tetrahedral site in the $Cd_{1-x}{}^{t}Mn(II)_x{}^{t}Mn(III)_2{}^{o}O_4$ with a negligible amount of structural cation vacancies can be regarded as reasonably proved by the experimental results here reported. At least at low temperature (i.e., below 500–600°C), this situation is commonly found in other direct spinel manganites such as $Mg_{1-x}{}^{t}Mn(II)_x{}^{t}Mn(III)_2{}^{o}O_4$, $Co_{1-x}{}^{t}Mn(II)_x{}^{t}Mn(III)_2{}^{o}O_4$, and $Zn_{1-x}{}^{t}Mn(II)_x{}^{t}Mn(III)_2{}^{o}O_4$ (12), but it is contrary to what is found in nickel manganese spinels. The last compound exhibits a more complex defect situation with (a) a considerable amount of vacancies in the tetrahedral site, (b) Mn(IV) in the octahedral site, and (c) a considerable amount of both Ni(II) and Ni(III) on the octahedral site, so that (d) there can be no Mn(III) in this site (12). This difference is reasonably explained by the fact that nickel manganese spinels are cubic, and Mn(IV) cannot present Jahn–Teller distortion, while Mn(III) is a typical Jahn–Teller ion.

Finally, it must be pointed out that XAS is a local probe: an XAS experiment at the Mn edges probes only the local chemical environment of Mn. Therefore, nothing can be said about the chemical environment of Cd, and, in particular, the presence of some amounts of Cd in sites other than the tetrahedral ones cannot be ruled out. This is a different problem that needs further experimental work, for example, involving XAS at the Cd–K edge.

REFERENCES

1. N. Yamazoe and N. Miura, *Solid State Ionics* **86–88,** 987 (1996).
2. N. Miura, G. Lu, N. Yamazoe, H. Kurosawa, and M. Hasei, *J. Electrochem. Soc.* **143,** L33 (1996).
3. N. Miura, H. Kurosawa, H. Hasei, G. Lu, and N. Yamazoe, *Solid State Ionics* **86–88,** 1069 (1996).
4. JCPDS-ICCD, 23-826, 1989.
5. A. P. B. Sinha, N. R. Sanjana, and A. B. Biswas, *Z. Kristallogr.* **109,** 410 (1957).
6. A. P. B. Sinha, N. R. Sanjana, and A. B. Biswas, *Acta Crystallogr.* **10,** 439 (1957).
7. G. Spinolo, G. Flor, G. Chiodelli, N. Barbi, and P. Ghigna, in preparation.
8. A. Filipponi, A. Di Cicco, and C. R. Natoli, *Phys. Rev. B* **52,** 15122 (1995).
9. A. Filipponi, and A. Di Cicco, *Phys. Rev. B* **52,** 15135 (1995).
10. B. D. Padalia and V. Krishnan, *Phys. Status Solidi* **a25,** K177 (1974).
11. B. D. Padalia, V. Krishnan, M. J. Patni, N. K. Radhakrishnan, and S. N. Gupta, *J. Phys. Chem. Solids* **24,** K173 (1973).
12. C. Laberty, M. Verelst, P. Lecante, P. Alphonse, A. Mosset, and A. Rousset, *J. Solid State Chem.* **129,** 271 (1997).